

The Anderson Transition in Lattice QCD

Robin Kehr

Institute for Theoretical Physics,
Justus Liebig University Giessen

Lunch Club Seminar – February 14, 2024



Based on:

R. Kehr, D. Smith, L. von Smekal, arXiv:2304.13617

- 1 Motivation
- 2 QCD on the lattice
- 3 Numerical methods and lattice setup
- 4 Results and analysis
- 5 Conclusion and outlook

- 1 Motivation
- 2 QCD on the lattice
- 3 Numerical methods and lattice setup
- 4 Results and analysis
- 5 Conclusion and outlook

Motivation

- Principal transitions within the QCD phase diagram:
Chirally broken \rightarrow Chirally restored & Confined \rightarrow Deconfined phase

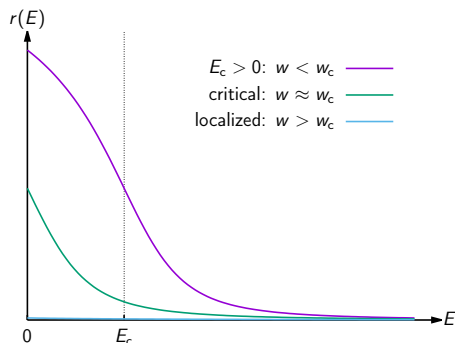
Open question

Is chiral symmetry breaking related to confinement and if so, how?

- QCD Anderson transition seems to be **related to both phenomena**
 \Rightarrow Might provide the answer to this question
- In this work: Focus on relation to chiral symmetry breaking
- Term *Anderson transition* originates from condensed matter physics
[P. W. Anderson, 1958] [F. Evers, A. D. Mirlin, arXiv:0707.4378]
 - Describes metal-insulator transition in disordered solids
 - In metal phase **low-lying** eigenmodes of Hamiltonian are **delocalized**
 \Rightarrow Conductivity
 - Above critical disorder all eigenmodes **localized** \Rightarrow No conductivity

Anderson transition

- Delocalized modes separated from localized modes by energy threshold E_c (*mobility edge*)
- Above critical disorder strength w_c all modes are localized



- Similar transition in QCD [M. Giordano, T. G. Kovács, arXiv:2104.14388]
 - Hamilton operator
→ Dirac operator
 - Disorder strength
→ Temperature
 - Low-lying modes are localized
 - Higher ones delocalized
 - Below T_0 all modes are delocalized (no mobility edge)

... (de)confinement

- Eigenmodes tend to localize in the sinks of Polyakov loop [L. Holicki, E.-M. Ilgenfritz, L. von Smekal, arXiv:1810.01130]
- In quenched QCD the vanishing of mobility edge coincides with the deconfining phase transition [T. G. Kovács, R. Á. Vig, arXiv:1706.03562]

... chiral symmetry restoration/breaking

- Previous work suggests $T_0 = T_{pc}$, where T_{pc} is the pseudocritical temperature of the chiral crossover (nonvanishing quark mass)
- No Goldstone bosons in the chiral limit, if near-zero modes are localized [M. Giordano, arXiv:2206.11109]
 $\Rightarrow T_0 \geq T_c$ (T_c : temperature of the chiral phase transition)
- Near-zero modes **produce chiral condensate** (Banks-Casher relation)
[T. Banks, A. Casher, 1980]

Outline

- 1 Motivation
- 2 QCD on the lattice
- 3 Numerical methods and lattice setup
- 4 Results and analysis
- 5 Conclusion and outlook

QCD in the continuum

- QCD expectation value:

$$\langle O \rangle = \frac{1}{\mathcal{Z}} \int_{\mathcal{C}} \mathcal{D}[\psi, \bar{\psi}, A] O[\psi, \bar{\psi}, A] e^{-S[\psi, \bar{\psi}, A]}$$

- Partition function:

$$\mathcal{Z} = \int_{\mathcal{C}} \mathcal{D}[\psi, \bar{\psi}, A] e^{-S[\psi, \bar{\psi}, A]}$$

- Action: $S[\psi, \bar{\psi}, A] = S_F[\psi, \bar{\psi}, A] + S_G[A]$

- Gauge action for **finite temperature** T (Euclidean):

$$S_G[A] = \frac{1}{2g^2} \int_0^{\frac{1}{T}} dt \int_{\mathbb{R}^3} d^3\vec{x} \operatorname{tr}(F_{\mu\nu}(x)F_{\mu\nu}(x))$$

- Fermion action:

$$S_F [\psi, \bar{\psi}, A] = \int_0^{\frac{1}{T}} dt \int_{\mathbb{R}^3} d^3 \vec{x} \bar{\psi}(x) D_c(x) \psi(x)$$

Dirac operator

$$D_c(x) = \gamma_\mu (\partial_\mu + i A_\mu(x)) + m$$

- Anticommutates with γ_5 for $m = 0$:

$$\{D_c|_{m=0}, \gamma_5\} = 0$$

- Massless action invariant under chiral rotations:

$$\psi \mapsto \exp(i\alpha \gamma_5) \psi$$

$$\bar{\psi} \mapsto \bar{\psi} \exp(i\alpha \gamma_5)$$

Fermion action on the lattice

- Want to **keep symmetries** of continuum action if possible
 - Discretize four-dimensional spacetime (with lattice spacing a)
 - Central difference quotient for the partial derivative
-
- Naive discretization of the fermion action:

$$S_{\text{naive}} [\psi, \bar{\psi}, U] = a^4 \sum_{n \in \Lambda} \bar{\psi}(n) \left(m\psi(n) + \gamma_{\mu} \frac{U_{\mu}(n)\psi(n + e_{\mu}) - U_{-\mu}(n)\psi(n - e_{\mu})}{2a} \right)$$

Group valued link variables

$$U_{\mu}(n) = \exp(i a A_{\mu}(n))$$

- Negative direction:

$$U_{-\mu}(n) := U_{\mu}(n - e_{\mu})^{\dagger}$$

Doubling problem

- Read off lattice Dirac operator:

$$S_{\text{naive}} [\psi, \bar{\psi}, U] = a^4 \sum_{n, l \in \Lambda} \bar{\psi}(n) D_{\text{naive}}(n, l) \psi(l)$$

- Consider free naive Dirac operator ($U_\mu \equiv \mathbb{1}$)
- Take Fourier transform and invert

Free naive fermion propagator

$$\tilde{D}_{\text{naive}}^0(p)^{-1} \Big|_{m=0} = \frac{-ia \gamma_\mu \sin(p_\mu a)}{\sum_{\nu=1}^4 \sin^2(p_\nu a)} \xrightarrow{a \rightarrow 0} \frac{-i\gamma_\mu p_\mu}{p^2}$$

- Correct continuum limit but $2^4 = 16$ poles:

$$p = a^{-1} (p_1, p_2, p_3, p_4) \quad \text{with} \quad p_\mu \in \{0, \pi\}$$

- Wilson Dirac operator (momentum space):

$$\tilde{D}_W^0(p) = \tilde{D}_{\text{naive}}^0(p) + \underbrace{\frac{1}{a} \sum_{\mu=1}^4 (1 - \cos(p_\mu a))}_{\text{Wilson term}}$$

- Removes fermion doublers
- Vanishes for physical pole $p = (0, 0, 0, 0)$

- Wilson operator in position space ($\gamma_{-\mu} := -\gamma_\mu$):

$$D_W(n, l) = \left(m + \frac{4}{a}\right) \delta_{n,l} - \frac{1}{2a} \sum_{\mu=\pm 1}^{\pm 4} (1 - \gamma_\mu) U_\mu(n) \delta_{n+e_\mu, l} \sigma_\mu(n_4)$$

Chiral symmetry on the lattice

- From now $m=0 \Rightarrow$ Wilson operator still breaks chiral symmetry:

$$\{D_W, \gamma_5\} \neq 0$$

- Nielsen-Ninomiya theorem:
Chiral symmetric **and** doubler free lattice action does not exist!

- Ginsparg-Wilson equation:

$$\{D, \gamma_5\} = aD\gamma_5D \Leftrightarrow D\gamma_5\left(1 - \frac{a}{2}D\right) + \left(1 - \frac{a}{2}D\right)\gamma_5D = 0$$

- Modify chiral rotations:

$$\begin{aligned}\psi &\mapsto \exp\left(i\alpha\gamma_5\left(1 - \frac{a}{2}D\right)\right)\psi \\ \bar{\psi} &\mapsto \bar{\psi}\exp\left(i\alpha\left(1 - \frac{a}{2}D\right)\gamma_5\right)\end{aligned}$$

Ginsparg-Wilson fermions

- Consider γ_5 -hermitian Dirac operator:

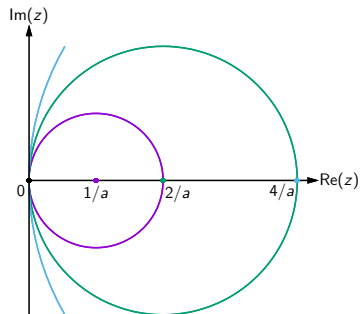
$$\gamma_5 D \gamma_5 = D^\dagger$$

\Rightarrow Eigenvalues are either real or come in complex conjugate pairs

- Ginsparg-Wilson equation:

$$v_\lambda \text{ eigenmode with eigenvalue } \lambda \quad \Rightarrow \quad v_{\lambda^*} = \gamma_5 v_\lambda$$

- γ_5 -hermiticity and Ginsparg-Wilson equation:
 \Rightarrow Eigenvalues lie on circle in complex plane with center at $1/a$ and radius $1/a$ (Ginsparg-Wilson circle)



Overlap operator

$$D_{\text{ov}} = \frac{1}{\tilde{a}} (1 + \text{sgn } K)$$

- γ_5 -hermitian kernel operator K :

$$\gamma_5 K \gamma_5 = K^\dagger \quad \Rightarrow \quad \text{sgn } K = \frac{K}{\sqrt{K^\dagger K}} \quad \text{is well defined}$$

- In this work:

$$K = aD_W - (1 + s)$$

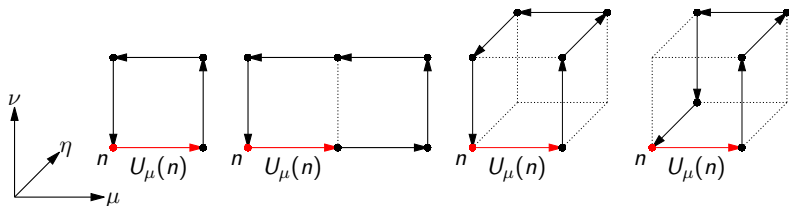
- Let $\tilde{a} = a/(1 + s)$:

$$\Rightarrow D_{\text{ov}} \xrightarrow{a \rightarrow 0} D_C$$

- Not strictly local due to inverse square root
- Still exponential decay:

$$\|D_{\text{ov}}(n, l)\| \leq C \exp(-c \|n - l\|)$$

Lattice gauge action



- Plaquette:

$$P_{\mu\nu}(n) = U_\mu(n) U_\nu(n + e_\mu) U_\mu(n + e_\nu)^\dagger U_\nu(n)^\dagger$$

- Wilson gauge action:

$$S_W[U] = \frac{2}{g^2} \sum_{n \in \Lambda} \sum_{\mu < \nu} \text{Re tr}(\mathbb{1} - P_{\mu\nu}(n))$$

Expectation value on the lattice

- Rearrange and integrate out fermions:

$$\langle O \rangle = \frac{1}{\mathcal{Z}} \int_{\mathcal{C}_G} \mathcal{D}[U] e^{-S_G[U]} \mathcal{Z}_F[U] \langle O \rangle_F[U]$$

- Measure for gauge field:

$$\mathcal{D}[U] = \prod_{n \in \Lambda} \prod_{\mu=1}^4 dU_{\mu}(n)$$

- Generate set of gauge field configurations U_1, U_2, \dots, U_k :

$$dP[U] = \frac{1}{\mathcal{Z}} \mathcal{D}[U] e^{-S_G[U]} \mathcal{Z}_F[U]$$

- Fermion determinant:

$$\mathcal{Z}_F[U] = -a^4 \det(D)$$

- Approximate path integral by Monte Carlo simulation:

$$\langle O \rangle \approx \frac{1}{k} \sum_{i=1}^k \langle O \rangle_F[U_i]$$

- 1 Motivation
- 2 QCD on the lattice
- 3 Numerical methods and lattice setup**
- 4 Results and analysis
- 5 Conclusion and outlook

Implementation of the overlap operator

- High-dimensional matrix:

$$d = \underbrace{4}_{\text{Dirac}} \cdot \underbrace{3}_{\text{color}} \cdot \underbrace{\prod_{\mu=1}^4 N_{\mu}}_{\text{lattice sites}}$$

- $N_s = 24$, $N_t = 4$: $d \approx 660$ k
 $\Rightarrow d^2 \approx 440$ billion complex entries $\hat{\approx}$ 3.2 TB storage (single precision)
- $N_s = 48$, $N_t = 20$: $\hat{\approx}$ 5 PB
- **No chance of storing the whole operator!**

- Implement matrix-vector product $D_{ov}v$ instead
- Rational approximation for sign function:

$$\text{sgn } K = \frac{1}{\sqrt{(\gamma_5 K)^2}} \\ \approx \alpha_0 + \sum_{j=1}^k \frac{\alpha_j}{(\gamma_5 K)^2 + \beta_j}$$

- Solve system of equations $\forall j$:

$$((\gamma_5 K)^2 + \beta_j) w_j = v$$

- Conjugate gradient method

Krylov subspace methods

- Due to high dimension **entire diagonalization not feasible!**
- Compute small part of spectrum using Krylov subspace methods

- p -dimensional Krylov subspace to matrix A and start vector x_1 :

$$\mathcal{K}_p(A, x_1) = \text{span}\{x_1, Ax_1, A^2x_1, \dots, A^{p-1}x_1\}$$

- Let u_1, u_2, \dots, u_p be an orthonormal basis of the Krylov subspace
- Projection onto subspace:

$$H = U^\dagger AU$$

- Compute eigenvalues θ_i and eigenvectors y_i of H
- Approximate eigenpairs of A :
 $\lambda_i \approx \theta_i$ (Ritz values)
 $v_i \approx Uy_i$ (Ritz vectors)
- Best approximations in $\mathcal{K}_p(A, x_1)$

Arnoldi method

- Successively extend Krylov subspace with $\omega := Au_j$
- Compute matrix elements $H_{ij} = u_i^\dagger \omega$
- Orthogonalize ω to u_1, u_2, \dots, u_j
- Compute $H_{j+1,j} = \|\omega\|_2$ and set $u_{j+1} = \omega / \|\omega\|_2$

- H takes upper Hessenberg form of dimension p
- Arnoldi decomposition:

$$AU = UH + (Au_p) e_p^\dagger$$

- Krylov decomposition:

$$AU = UB + u_{p+1} b_{p+1}^\dagger$$

- **Krylov-Schur:** B has 1×1 or 2×2 blocks on the diagonal

Repeat

- Build Krylov decomposition using Arnoldi method
- Transform into Krylov-Schur decomposition
- Reorder blocks according to desired eigenvalues
- Truncate Krylov subspace

Mixed action setup

- Compute low-lying eigenmodes of overlap operator with Wilson kernel:

$$D_{\text{ov}} = \frac{1+s}{a} (1 + \text{sgn } K), \quad \text{where } K = aD_W - (1+s)$$

- Configurations from *twisted mass at finite temperature* collaboration [F. Burger, E.-M. Ilgenfritz, M. P. Lombardo, A. Trunin, arXiv:1805.06001]
 - Twisted mass Wilson fermions at maximal twist, Iwasaki gauge action
 - $N_f = 2 + 1 + 1$: two degenerate light & physical strange, charm quarks
 - Pseudocritical temperature T_{pc} from disconnected chiral susceptibility
 - Lattice spacing a from nucleon mass [C. Alexandrou et al., arXiv:1406.4310]
- Mixed action setup well studied [K. Cichy et al., arXiv:1211.1605]
 - Adopting lattice spacing a and matching quark mass (respectively m_π)
 \Rightarrow Consistent continuum limit for f_π , m_N and m_Δ
 - Locality: $s = 0.4$ optimal value for $N_f = 2$ and Symanzik gauge action

Gauge configurations

Set of ensembles	N_s	N_t	T / MeV	T / T_{pc}	# conf.	$\frac{\text{modes}}{\text{conf.}}$	
A370 $a = 0.0936(13) \text{ fm}$ $m_\pi = 364(15) \text{ MeV}$ $T_{\text{pc}} = 185(8) \text{ MeV}$	24	4	527(7)	2.85(13)	200	200	
		5	422(6)	2.28(10)	200	160	
		6	351(5)	1.90(9)	200	135	
		7	301(4)	1.63(7)	150	115	
		8	264(4)	1.42(6)	200	100	
		9	234(3)	1.27(6)	200	90	
		10	211(3)	1.14(5)	250	80	
		11	192(3)	1.04(5)	200	75	
		12	176(2)	0.95(4)	200	70	
		32	13	162(2)	0.88(4)	50	150
			14	151(2)	0.81(4)	50	140
		D370 $a = 0.0646(7) \text{ fm}$ $m_\pi = 369(15) \text{ MeV}$ $T_{\text{pc}} = 185(4) \text{ MeV}$	32	3	1018(11)	5.50(13)	120
	6			509(6)	2.75(7)	120	200
	14			218(2)	1.18(3)	160	85
16	191(2)			1.03(2)	160	75	
40	18		170(2)	0.92(2)	40	150	
48	20		153(2)	0.83(2)	3	200	
D210 $a = 0.0646(7) \text{ fm}$ $m_\pi = 213(9) \text{ MeV}$ $T_{\text{pc}} = 158(5) \text{ MeV}$	48	4	764(8)	4.83(16)	10	1000	
		6	509(6)	3.22(11)	10	700	
		8	382(4)	2.42(8)	10	500	
		10	305(3)	1.93(6)	10	400	
		12	255(3)	1.61(5)	10	350	
		14	218(2)	1.38(5)	10	300	
		16	191(2)	1.21(4)	10	250	
		18	170(2)	1.07(4)	10	225	
		20	153(2)	0.97(3)	-	-	
		24	127(1)	0.81(3)	-	-	

- N_s : Number of lattice sites in each space direction

- Volume = L^3 :

$$L = aN_s$$

- N_t : Number of lattice sites in temporal direction

- Temperature:

$$T = \frac{1}{aN_t}$$

Outline

- 1 Motivation
- 2 QCD on the lattice
- 3 Numerical methods and lattice setup
- 4 Results and analysis**
- 5 Conclusion and outlook

Stereographic projection

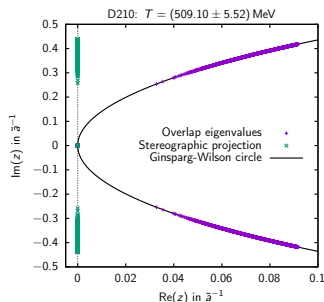
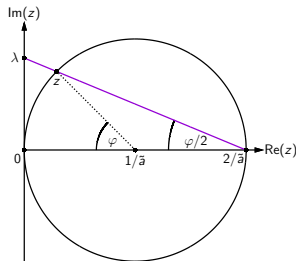
- Mimic continuum limit by projecting eigenvalues on imaginary axis
- Require $f(z) = z + \mathcal{O}(\tilde{a}z^2)$ and $f(2/\tilde{a}) = \infty$ [W. Bietenholz, K. Jansen, S. Shcheredin, arXiv:0306022]:

$$f(z) = \frac{z}{1 - \frac{\tilde{a}}{2}z}$$

(Möbius transformation)

- Translates to stereographic projection:

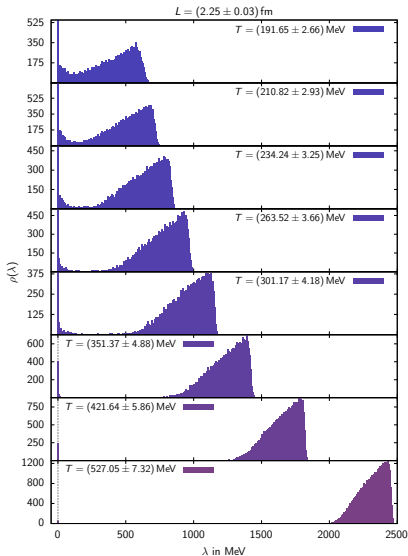
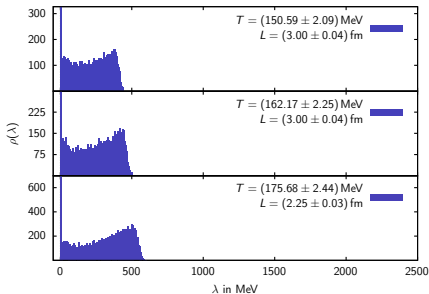
$$\lambda := f(\lambda) = \frac{i \operatorname{Im} \lambda}{1 - \frac{\tilde{a}}{2} \operatorname{Re} \lambda} = i \frac{2}{\tilde{a}} \tan \frac{\varphi}{2}$$



Distribution A370: $a = 0.0936(13)$ fm, $m_\pi = 364(15)$ MeV

- Banks-Casher relation:

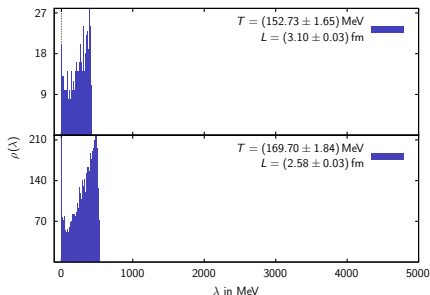
$$\langle \bar{\psi}\psi \rangle = -\pi \lim_{\lambda \rightarrow 0} \lim_{m \rightarrow 0} \lim_{V \rightarrow \infty} \rho(\lambda)$$



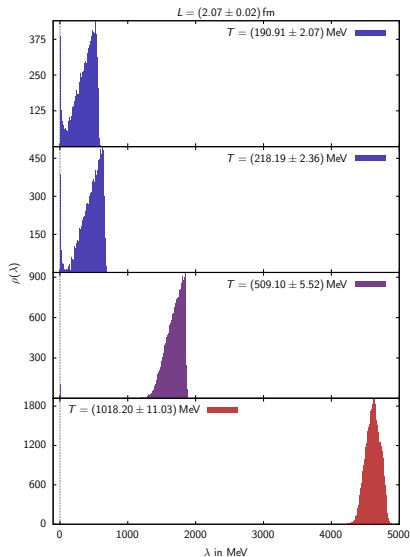
- $T_{pc} = 185(8)$ MeV

Distribution D370: $a = 0.0646(7)$ fm, $m_\pi = 369(15)$ MeV

- Roughly same m_π , T_{pc} and volume but **smaller lattice spacing a**



- $T_{pc} = 185(4)$ MeV

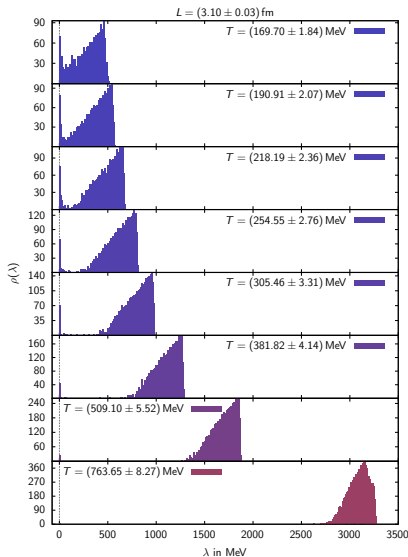


Distribution D210: $a = 0.0646(7)$ fm, $m_\pi = 213(9)$ MeV

- Keep a but **reduce m_π , T_{pc}** and **increase volume**
- However smallest $m_\pi L \approx 3.3$ (at least > 3 , optimally > 4)

- $T_{pc} = 158(5)$ MeV

- Near-zero modes do not instantly vanish when increasing T above T_{pc} (chiral crossover)
- For increasing temperature an increasingly wider gap emerges (Banks-Casher gap)



Localization measure

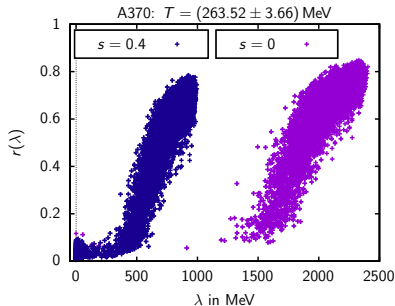
- Need **measure of localization** to reveal QCD Anderson transition
- Relative eigenmode volume:

$$r(\lambda) = \frac{P_2^{-1}(\lambda)}{|\Lambda|} \in [1/|\Lambda|, 1]$$

with *inverse participation ratio*

$$P_2(\lambda) = \sum_{i \in \Lambda} (v_\lambda(i)^\dagger v_\lambda(i))^2$$

- Maximally localized on n_0 :
 $v_\lambda(n)^\dagger v_\lambda(n) = \delta_{n,n_0}$
 $\Rightarrow r(\lambda) = 1/|\Lambda|$
- Maximally delocalized:
 $v_\lambda(n)^\dagger v_\lambda(n) = 1/|\Lambda|$
 $\Rightarrow r(\lambda) = 1$



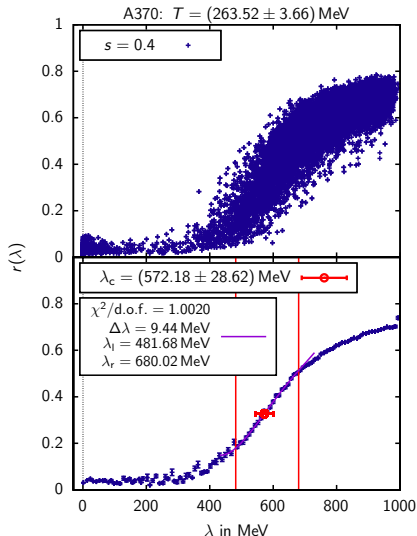
- Transition clearly visible
- Need criterion to quantify position $\hat{=}$ **mobility edge**
- Employ inflection point (IP)

Strategy for determining the IP

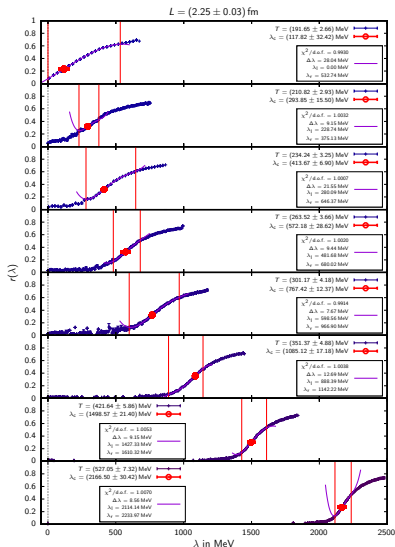
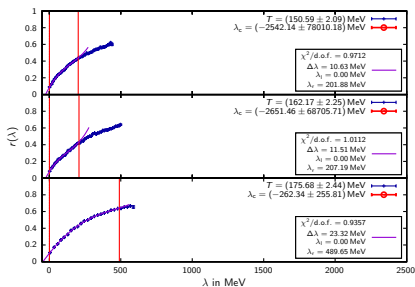
- Average over small bins in λ (\approx expectation value of $r(\lambda)$)
- Obtain data with standard error
- Vary binsize and fit window
- Find fits with $\chi^2/\text{d.o.f.} \approx 1$
- Read off inflection point

Fit Taylor polynomial (at IP)

$$r(\lambda) = r_c + b(\lambda - \lambda_c) + 0(\lambda - \lambda_c)^2 + c(\lambda - \lambda_c)^3 + d(\lambda - \lambda_c)^4$$

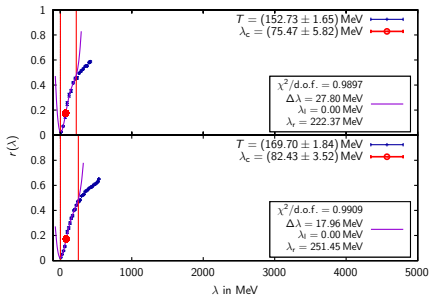


A370: $a = 0.0936(13)$ fm, $m_\pi = 364(15)$ MeV



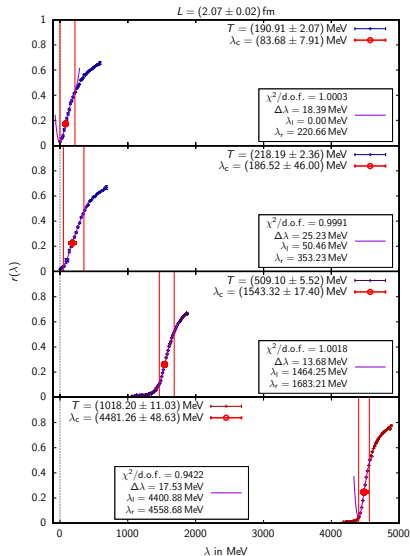
- Mobility edge vanishes below $T_{pc} = 185(8)$ MeV
- Consistent with earlier work [M. Giordano et al., arXiv:1410.8392] [L. Holicki, E.-M. Ilgenfritz, L. von Smekal, arXiv:1810.01130]

- Smaller lattice spacing a



- Mobility edge **does not** vanish below

$$T_{pc} = 185(4) \text{ MeV}$$



D210: $a = 0.0646(7)$ fm, $m_\pi = 213(9)$ MeV

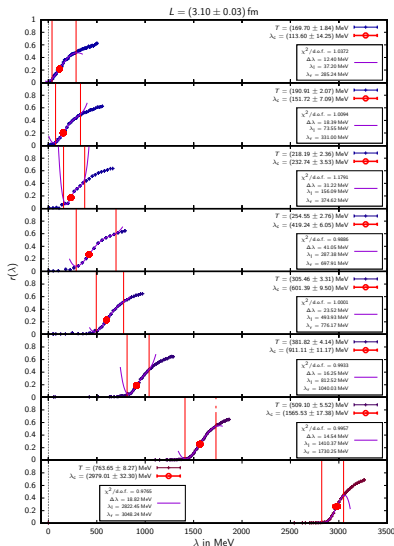
- Move closer towards physical limit: reduce m_π , T_{PC} , increase volume

- Find mobility edge for all evaluated ensembles, but **all** temperatures are **above**

$$T_{\text{PC}} = 158(5) \text{ MeV}$$

Key question

Where does the mobility edge vanish in the physical limit?

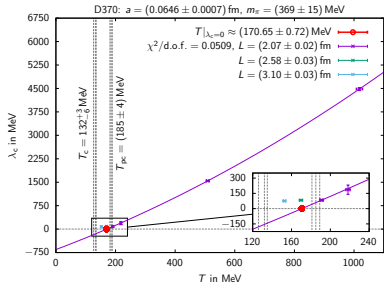
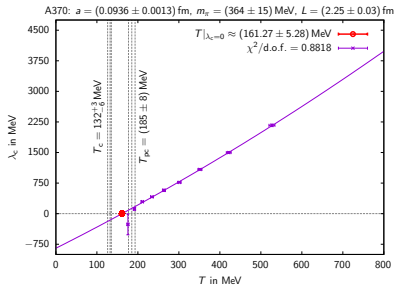


Temperature extrapolation of the mobility edge

Fit Taylor polynomial (at the zero)

$$\lambda_c(T) = b(T - T_0) + c(T - T_0)^2$$

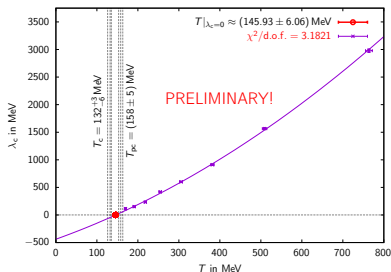
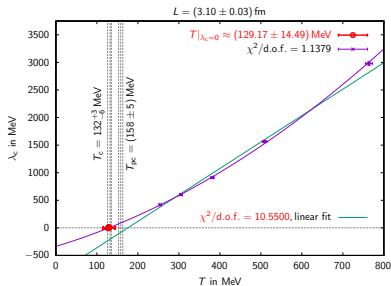
- A370 consistent with linear dependence and vanishing at T_{pc} as seen in earlier work [L. Holicki, E.-M. Ilgenfritz, L. von Smekal, arXiv:1810.01130]
- D370 shows slight curvature and no vanishing at T_{pc} , supported by data points to larger volumes
- In [M. Giordano et al., arXiv:1410.8392] actually slight curvature as well



Extrapolation D210: $a = 0.0646(7)$ fm, $m_\pi = 213(9)$ MeV

- Linear fit breaks down
- There is definitely a **curvature**
- Zero **coincides with T_c** ($m \rightarrow 0$)
[H.-T. Ding et al., arXiv:1903.04801]
- Data still far away from T_{pc} & T_c

- Include lower temperatures
- T_0 gets slightly shifted upwards but still below T_{pc}
- Bad $\chi^2/\text{d.o.f.}$ and e.g. fit for $T = 218(2)$ MeV not convincing
 \Rightarrow Better statistics and/or analysis needed

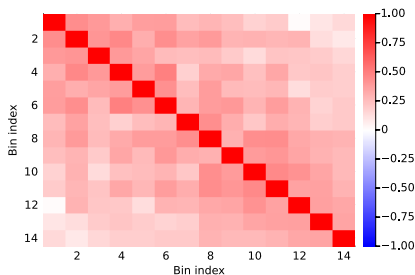
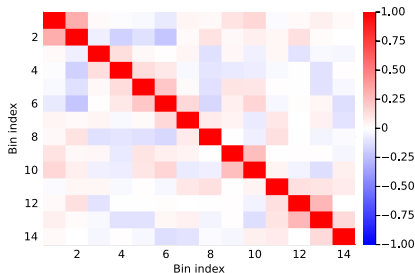


Correlation analysis

- Criterion $\chi^2/\text{d.o.f.} \approx 1$ requires statistically independent errors
- **Same** configurations for each bin
 \Rightarrow Bins might be correlated
- Quantify by computing Pearson correlation coefficient of bin X and Y :

$$\rho_{X,Y} = \frac{\text{cov}(X, Y)}{\sigma_X \sigma_Y}$$

- Correlation of λ (top) and $r(\lambda)$ (bottom) for $N_t = 4$ of A370
- Correlations for λ negligible
but not for $r(\lambda)$

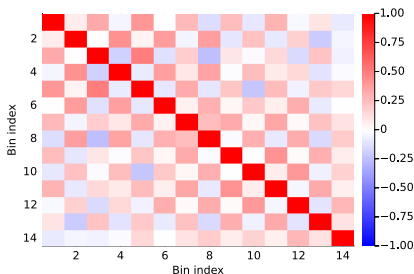
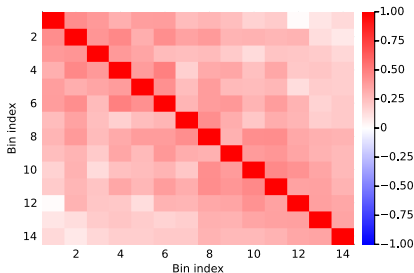


Reduce correlation

- Correlation especially strong for **neighboring** bins
 - ⇒ Pick different configurations:
Even index for bin i , odd for bin $i + 1$ (alternate picking)
- Correlation for relative volume strongly reduced (bottom)

- Repeat analysis with new method
- Small difference (a for alternating)

Data set	T_0 / MeV	$T_{0,a}$ / MeV
A370	161(5)	158(6)
D370	171(1)	168(2)
D210	129(14)	137(9)



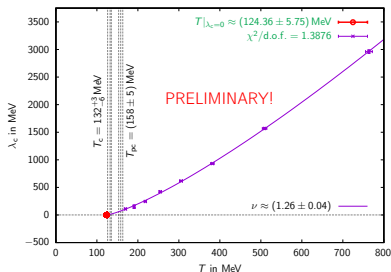
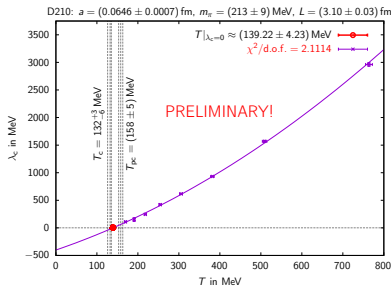
Scaling (second order phase transition)?

- Repeat quadratic fit for D210
- T_0 gets shifted downwards again
- Better $\chi^2/\text{d.o.f.}$ but still not convincing

- Try scaling fit:

$$\lambda_c(T) = b(T - T_0)^\nu$$

- T_0 moves downwards **back to T_c**
- **Acceptable $\chi^2/\text{d.o.f.}$** , however **just 5** configurations per bin
- $\nu \approx 1.437$ for unitary Anderson model [L. Ujfalusi, I. Varga, arXiv:1501.02147]



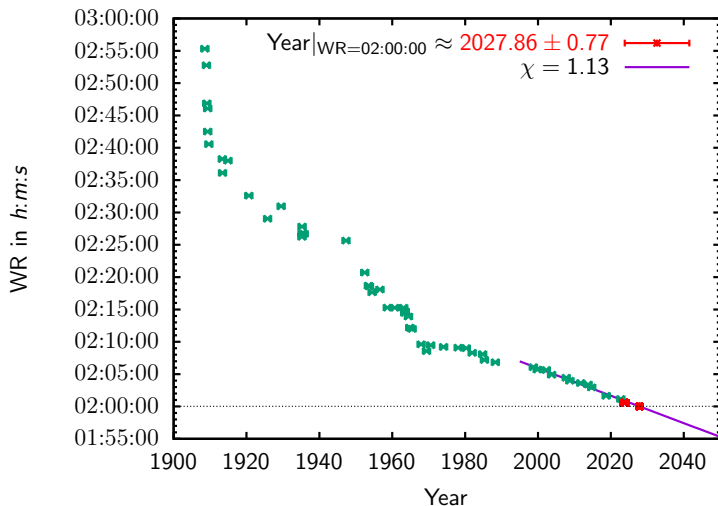
Outline

- 1 Motivation
- 2 QCD on the lattice
- 3 Numerical methods and lattice setup
- 4 Results and analysis
- 5 Conclusion and outlook

Conclusion and outlook

- Mobility edge λ_c depends **nonlinear** on the temperature (scaling?)
- Evidence for vanishing of λ_c at T_c and especially **not at T_{pc}**
- Data on lower temperatures and closer to physical limit necessary
*** \Rightarrow Reduce computational costs**
 - Improve program (if possible)
 - Apply UV-smoothing to lattice gauge configurations
- Employ other definitions of localization [A. Alexandru, I. Horváth, arXiv:2103.05607] \Rightarrow Find **infrared** mobility edge ***(...)**
- **Annihilation** of both mobility edges as alternative scenario
- Both scenarios combined possible as well
- Determine mobility edge more precisely by finite-size analysis ***(...)**
- Study correlation of eigenmodes with Polyakov loop

Extra: (Official) Marathon world record extrapolation



⇒ Magical two hour mark will be broken in **2028(1)**!

Thank you!